Low Temperature Physics/Fizika Nizkikh Temperatur, 2021, vol. 47, No. 12, pp. 1157–1164

Desorption of excited H^* atoms from free clusters Ar/CH_4 and solid Ar doped with CH_4

Yu. S. Doronin, V. L. Vakula, G. V. Kamarchuk, A. A. Tkachenko, I. V. Khyzhniy, S. A. Uyutnov, M. A. Bludov, and E. V. Savchenko

B. Verkin Institute for Low Temperature Physics and Engineering of NAS of Ukraine, Kharkiv 61103, Ukraine
E-mail: doronin@ilt.kharkov.ua

Received August 13, 2021, published online October 25, 2021

Desorption of excited hydrogen atoms was detected from both solid Ar doped with CH_4 and free nanoclusters Ar/CH_4 at irradiation with an electron beam. It was monitored by an emission of the Lyman-α line. Measurements of cathodoluminescence (CL) spectra in the VUV range were performed within the CH_4 concentration limits 0.1–10 % in the solid matrix. The CL of free clusters with an average size of 1200 atoms per cluster was detected from pure Ar cluster jet and from Ar clusters doped with 0.1% CH_4. The mechanisms of desorption of electronically excited H^* atoms from solids and clusters are proposed on the basis of an analysis of energy transfer pathways with the final stage of relaxation — population of the $n = 3$ state of hydrogen atoms.

Keywords: methane, hydrogen, matrix isolation, clusters, electron irradiation, luminescence, desorption.

1. Introduction

Methane attracted particular interest in many fields of science. Being the simplest compound from the hydrocarbon family it was discussed from the point of view of prebiotic chemistry [1]. One more field of interest is related to the behavior of solid methane under neutron flux. Despite high efficiency of the conversion of short wavelength neutrons to long wavelength ones (3.5 times higher than that achieved in liquid hydrogen based moderators) [2] its application encounters some difficulties. It turned out that a neutron flux can cause spontaneous release of accumulated energy and rapid heating followed by hydrogen expansion and moderator destruction. This phenomenon received a further look [3–7]. Methane and methane-containing systems as important constituents of Interstellar Medium and Solar System have been widely studied by astrophysicists for many years (see, e.g., [8–23]). Studies of matrix-isolated methane are not so numerous. Methane was studied in Kr matrix under photolysis using synchrotron VUV radiation [24]. Neon matrix was used in works on photolysis of methane at low temperatures [15, 25–27]. Radiation effects in methane-doped Ar matrix were investigated when excited with an electron beam [28–30].

An essential feature of the methane molecule CH_4 is the instability of its electronically excited states, i.e., methane in excited states tends to dissociate into fragments, which can be studied by FTIR spectroscopy or identified by their emission spectra. Main channels of CH_4 degradation (see [31], where results of numerous studies were compiled) are:

$$CH_4 \rightarrow CH_3+H, \quad (1)$$

$$CH_4 \rightarrow CH_2+H_2, \quad (2)$$

$$CH_4 \rightarrow CH_2+2H, \quad (3)$$

$$CH_4 \rightarrow CH+H+H_2. \quad (4)$$

The main products of these reactions and reactions of secondary products fragmentation are atomic and molecular hydrogen. H atoms which are formed in reactions (1), (3), and (4) have an excess of kinetic energy, e.g., in channel (1) the experimental mean kinetic energy of the neutral lighter fragment H appeared to be 3.1 eV [32]. In most other channels this energy exceeds 1 eV and such "fast" H atoms may diffuse for quite a long distance. After thermalization the H atoms occupy two types of sites in Ar lattice — octahedral interstitial site and substitutional one [33, 34]. The atoms occupying the interstitial sites are released at moderate heating, while the atoms trapped in the substitutional sites remain trapped [35]. H atoms trapped in CH_4-doped Ar matrices irradiated with an electron beam were observed in [28] by the emission band at 166 nm, which belongs to the excimer $(Ar_2H)^*$ [36]. It was found that the intensity of this band decreased 5 times with increasing methane concentration from 1% to 5%. This implies a more rapid depletion of atomic hydrogen at higher concentrations due to its diffusion followed by

nonradiative recombination of the H atoms with the release of energy and the formation of molecular hydrogen. In the study [28], desorption of excited hydrogen atoms was also detected by their emission of the Ly-α line. This phenomenon is of high interest for basic science and astrophysical research.

We continued our research on the desorption of electronically excited hydrogen atoms to highlight the underlying processes, and extended the study to free clusters Ar/CH_4 to get more insight into desorption processes at the nanoscale level. Gases of the same purity were used to prepare solid samples and clusters. In experiments of both types, with solid matrices and with clusters, electrons of close energy were used. The spectra were measured in the VUV range, and their transformation caused by an admixture of methane was investigated with an emphasis on the size effect.

2. Experimental

2.1. *Solid* Ar *matrices doped with* CH_4

Experiments with solid Ar matrices doped with methane were performed using the setup described in detail in Sec. 7 of Ref. 37. Mixture of Ar and CH_4 of chosen concentration was performed in the gas-handling system which was heated and degassed before each experiment. We used Ar gas (99.998%) and CH_4 gas (99.97%) without further purification. Samples of 25 μm thickness were grown by deposition of a certain amount of gas mixture onto a cooled to liquid helium (LHe) temperature oxygen free copper substrate mounted in a high-vacuum chamber with a base pressure of 10^{-5} Pa. Pumping out was performed by LHe cryogenic pump and magnetic discharge pump.

The irradiation was performed in dc regime with electrons of subthreshold energy to avoid the knock-on sputtering of samples as well as the knock-on formation of lattice defects. It should be noted that electronically induced creation of defects, which serve as traps for electrons in the Ar lattice, occurs in solid Ar [38, 39]. The electron beam energy E_e was set to 1.5 keV with the current density of 2.5 mA·cm^{-2}. The beam covered an icy sample with an area of 1 cm^2. When the beam was turned on, the increase in temperature of the sample did not exceed 0.4 K. The sample temperature was controlled with a Si sensor mounted on the surface of substrate.

Cathodoluminescence (CL) spectra were detected in the range 100–300 nm with $\Delta\lambda = 0.16$ nm. This region includes the main features of the emission spectrum of the matrix, as well as the band of atomic hydrogen localized in the bulk of matrix $(Ar_2H)^*$, and the Ly-α line of an excited hydrogen atom desorbing from the matrix. The presence of impurities in the samples was monitored by the luminescence spectra. Note, that spectra were not corrected for the spectral sensitivity of the optical system.

The preparation of experiments should take into account the effect of explosive delayed desorption, which was detected in the CH_4-doped Ar matrix [28–30] after prolonged irradiation with an electron beam. This effect was found to be similar to that detected in pure solid methane [23, 40, 41]. The effect of explosive desorption from the surface of solid methane exposed to an electron beam was discovered upon reaching a critical irradiation dose of ~ 100 eV per methane molecule. Two kinds of self-oscillations of temperature and radical concentration were detected with short and long periods. Theoretical treatment of the effect was done in [41]. With this in mind, we carried out experiments presented in this paper at subcritical dose.

2.2. *Free clusters* Ar/CH_4

Experiments with free Ar clusters doped with methane were carried out using the supersonic jet source [42] for cluster generation, which has been modified. We used gaseous argon (99.998% purity) and gaseous CH_4 (99.97% purity) without additional purification. The initial gas mixture was a mixture of Ar with CH_4, with the concentration of methane $C = 0.1\%$. To generate clusters of chosen size a conical supersonic nozzle was used with a throat diameter of 0.34 mm, a cone angle of 8.6°, and an area of the exit section relative to the throat consisted of 36.7. The pressure P_0 and the temperature T_0 of the gas mixture at the nozzle inlet were 0.1 MPa and 180–200 K, respectively. For gas jet pumping a cryogenic pump cooled with liquid hydrogen was used and pressure in the experimental chamber did not exceed 10^{-3} Pa. At a distance of 30 mm from the nozzle exit cluster beam was crossed by the 1 keV electron beam. The electron beam current was set to 20 mA. As it was already mentioned electrons of this energy cannot induce a knock-on defect formation and sputtering and only electronically stimulated processes are possible. CL spectra were recorded in the range of 100–200 nm with $\Delta\lambda = 0.16$ nm. The technique of the optical measurements of the VUV luminescence of clusters of rare elements in supersonic jets is described in more detail in [42, 43]. The temperature and size of the clusters were taken from the data on electron diffraction studies of pure Ar clusters for the same nozzle geometry [44] on the assumption that low methane concentrations do not significantly change these parameters. In the experiments the width of the size distribution ΔN corresponded to the average number N of atoms per cluster (atom/cluster) [45]. The chosen cluster size was of 1200 atom/cluster.

3. Results and discussion

3.1. *Solid* Ar *matrices doped with* CH_4

CL spectra of Ar matrices doped with CH_4 were measured at concentrations C = 0.1, 1, 5, and 10%. Figure 1 shows, as an example, the spectrum of CL in the VUV

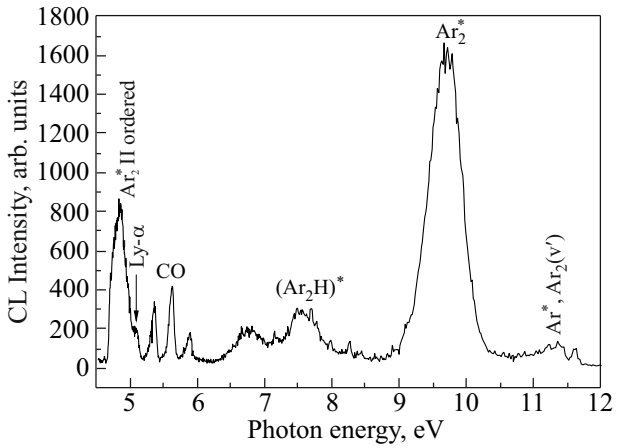

Fig. 1. VUV CL spectrum of Ar matrix doped with 1% CH_4 recorded at 1 keV electron beam excitation.

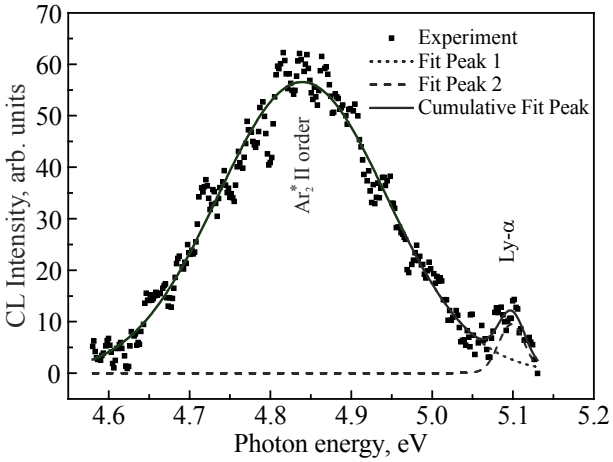

Fig. 2. Decomposition of the M-STE band recorded in the second spectral order. Peak 1 corresponds to the M-STE band, peak 2 corresponds to the Ly-α line recorded in the second spectral order. The resulting curve is shown together with the experimental points.

range taken from a 1% CH_4 matrix at 4.5 K. It was identical to that presented in [28, 30].

The spectrum consists of emission features of Ar matrix and radiolysis products – hydrogen in this spectral range. The most intense feature of this spectrum at 9.76 eV is the well-known emission of the molecular type self-trapped excitons (M-STE), corresponding to the transitions from $^{1,3}\Sigma_u^+$ states of Ar_2^* to a repulsive part of the ground state $^1\Sigma_u^+$ [46]. The radiative states of the self-trapped excitons can be populated via both the processes of exciton self-trapping and the recombination of the self-trapped hole (STH), that is (Ar_2^*), with an electron. Note that this band was also recorded in the second spectral order and we were able to detect on the high-energy side of this band the line of hydrogen atom emission at 5.1 eV (the Ly-α line in the second order). It should be mentioned that it is difficult to single out this line in the first order because of its overlap with the band of self-trapped excitons. The relevant part of the spectrum recorded in the second order is shown separately in Fig. 2. The experimental curve was fitted with two Gaussian curves (Fig. 2).

The coincidence of the peak 2 with the second order position of the Ly-α line in the gas phase indicates its connection with desorbing hydrogen atoms in the $n = 2$ electronically excited state. It is worthy of note that this line cannot stem from hydrogen atoms excited by electrons in the gas phase at such a pressure, 10^{-4} Pa. At excitation of pure solid methane with the same electron beam the Ly-α line was not observed. Weak features in the range between 11 and 12 eV belong to Ar atoms and molecules desorbing from the matrix surface in excited states. Hydrogen atoms appearing in the bulk manifest themselves by the emission of wide band at 7.47 eV, which has been assigned as the bound-free transitions of the excimer $(Ar_2H)^*$ [36]. The involvement of charged states in formation of excimers $(Rg_2H)^*$ and $(Rg_2D)^*$ was considered in [36, 47, 48]. These complexes were treated as the ion-pair states $(Rg_2^+H^-)$ and $(Rg_2^+D^-)$. The authors [49] suggested an exciton mechanism of D_2 dissociation which involves an intermediate complex $(RgD_2)^*$ formed due to localization of the matrix exciton near the D_2 impurity center. The spectrum also contains the Cameron system $a\,^3\Pi \rightarrow X^1\Sigma^+$ bands of CO and a broad band at 6.7 eV unidentified at present. Note, that this band disappeared at the CH_4 concentration C = 5%.

The intensity distribution in the spectra changed dramatically with changes in CH_4 concentration. Figure 3 demonstrates variation of the self-trapped excitons band Ar_2^*.

Such a strong quenching of the intrinsic matrix emission supposes that the energy transfer to dopants is accomplished by free carriers, which are thought to be free excitons and holes. It should be noted that the thickness of our samples d = 25 μm far exceeds the electron penetration depth r, which is $r \approx 100$ nm for 1.5 keV [50]. Thus, electrons excite directly only thin subsurface layer of the sample. The rest of Ar matrix (more than 99%) is excited by excitons

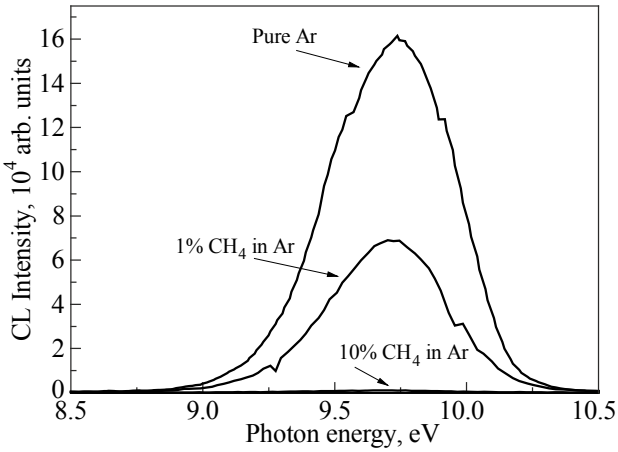

Fig. 3. Quenching of the intrinsic matrix emission, M-STE band, by doping with methane.

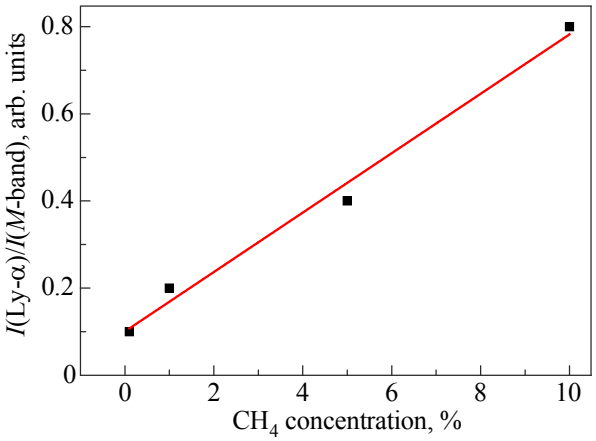

Fig. 4. Behavior of the relative intensity of the Ly-α line with the CH_4 concentration change.

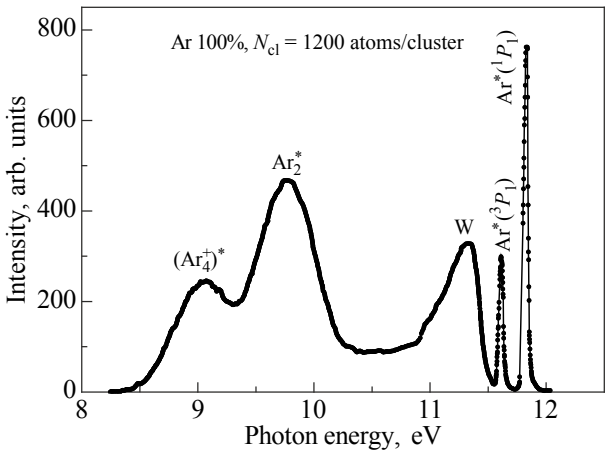

Fig. 5. VUV CL spectrum of Ar clusters with the average size $N \approx 1200$ atom/cluster recorded at 1 keV electron beam excitation and beam current of 20 mA.

and photons [30]. Under excitation above the band gap energy E_g one could expect a contribution of the charge recombination (neutralization) reaction to the formation of excimers.

An intensity of the excimer $(Ar_2H)^*$ band varies nonmonotonically with the methane concentration in Ar matrix. It grows with respect to the emission intensity of the matrix with an increase in the CH_4 concentration from 0.1% to 1%, and then decreases with an increase in the concentration of methane to 5%. The ratio $I(Ar_2H)^*/I(Ar_2^*)$ decreased 5 times with increasing methane concentration from 1% to 5%. This implies a more rapid depletion of atomic hydrogen at higher concentrations due to diffusion-controlled nonradiative recombination of H atoms with the energy release and the formation of molecular hydrogen.

In contrast to that the relative intensity of the desorbing atomic hydrogen I(Ly-α) with respect to the band of self-trapped excitons $I(Ar_2^*)$ varies monotonically with a methane concentration change in the range of 0.1–10%. It grows linearly with an increase in methane content as shown in Fig. 4.

It should be pointed out that the total yield of electron-induced desorption at subthreshold irradiation was not too high. The pressure in the experimental chamber registered in the dynamic pumping mode increased only by half the magnitude when the beam was switched on. In contrast to this the pressure burst at supercritical irradiation dose was several orders of magnitude higher [29, 40, 41].

3.2. Free clusters Ar/CH_4

In the first series of experiments CL spectra of pure Ar clusters were measured in the VUV range. Typical example of the CL spectra of free Ar clusters with the average size $N \approx 1200$ atoms/cluster (cluster diameter being 4.4 nm) is shown in Fig. 5. The most intense wide band (FWHM = = 0.6 eV) of clusters at 9.6 eV is similar to that observed in solid Ar which stems from the well-known emission of self-trapped excitons related to the bound-free $^{1,3}\Sigma_u^+ \rightarrow {}^1\Sigma_g^+$ transitions of the molecular dimer Ar_2^*. The second band at 8.9 eV has no analogue in the emission of solid Ar. It was assigned to radiative transitions in charged complexes $(Ar_4^+)^*$ [51, 52]. Detailed study [42] of the size effect in the CL spectra revealed that the neutral complexes Ar_2^* radiate from the whole volume of the cluster, while the charged complexes $(Ar_4^+)^*$ radiate from the near-surface layers of clusters.

The wide bands W at 10.6 and 11.3 eV belong to the vibrationally excited molecules $Ar_2^*(v')$ desorbing from the cluster surface. The narrow bands at 11.61 eV and 11.83 correspond to the $^3P_1 \rightarrow {}^1S_0$ and $^1P_1 \rightarrow {}^1S_0$ transitions in Ar atoms desorbing from clusters on exposure to the electron beam. These features were also observed in the bulk Ar solids [46] but with a much lower intensity.

Even small addition of methane, $C = 0.1\%$, into the gas mixture used for clusters generation resulted in strong modification of the CL spectrum. Bands of Ar_2^* and $(Ar_4^+)^*$ at 9.6 eV and 8.9 eV, respectively, appeared to be completely quenched as well as the wide bands at 10.6 and 11.3 eV belonging to the vibrationally excited molecules $Ar_2^*(v')$ desorbing from the clusters. The bands at 11.61 and 11.83 eV appeared to be strongly suppressed, in fact these remaining bands of Ar atoms stem from the gas component of the jet. The only feature detected in the range 8.5–10.5 eV turns out to be the Ly-α line. Its position 10.2 eV coincides with the position of this line in the gas phase, which indicates that hydrogen atoms are desorbed in an excited state and their emission occurs in the gas phase. Figure 6 shows the spectrum for mixed Ar/CH_4 clusters in the energy range 8.5–10.5 eV recorded under the same conditions which were used for the registration of CL from clusters of pure Ar: $P_0 = 0.1$ MPa and $T_0 = 180$–200 K.

An increase in the concentration C of CH_4 to $C = 0.5\%$ and a decrease in the initial pressure to 0.05 MPa resulted in an increase in the intensity of the Ly-α line by about 1.5 times.

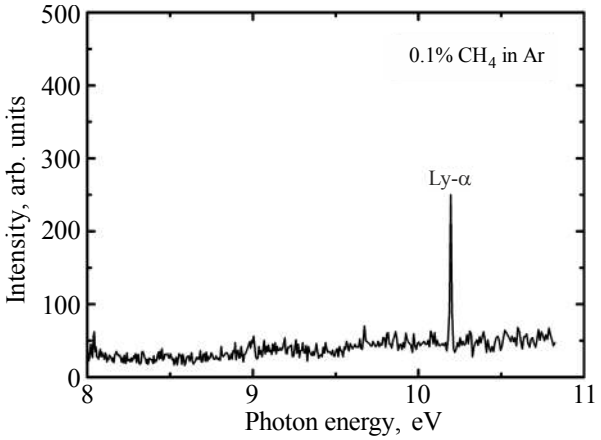

Fig. 6. CL spectrum of mixed Ar/CH_4 clusters under exposure to 1 keV electron beam. Pressure and temperature at the inlet of a nozzle were $P_0 = 0.1$ MPa and $T_0 = 180$–200 K, methane concentration in the initial mixture $C = 0.1\%$.

These experimental facts provide clear evidence that the mixed Ar/CH_4 clusters are formed in the jet, in which the impurity CH_4 molecules effectively intercept the excitation from the Ar environment.

3.3. Discussion

Electronically stimulated desorption occurs due to conversion of electronic excitation energy into kinetic energy of atoms. A necessary condition is the localization of electronic excitation on the hydrogen atom in the near-surface region with the release of energy exceeding the binding energy per atom ε_b (for atom of Ar matrix $\varepsilon_b = 88.8$ meV [46]). For the case of Ar matrix desorption of excited H^* atoms as well as excited atoms Ar^* of the matrix is facilitated by the negative electron affinity of Ar $\chi = -0.4$ eV [46], in other words, excited atoms are ejected under the repulsive forces between an excited atom and atoms of surrounding lattice.

Despite the close energies of exciting electrons in experiments with clusters and solid films, the excitation conditions turned out to be different. The practical range r of 1 keV electrons in Ar lattice ($r = 20$ nm [50]) exceeds the cluster's diameter $\delta = 4.4$ nm (at $N = 1.2 \cdot 10^3$ atom/cluster), while in solid films the practical range r of 1.5 keV incident electrons $r \sim 100$ nm is much less than the films thickness $d = 25$ μm. This results in an electron trapping and the accumulation of excess negative charge in the Ar matrix [54]. It has been shown [30] that because of the small penetration depth of electrons the bulk of the matrix is excited preferentially by free excitons and photons with an energy of 9.76 eV, the most intense emission band of the matrix (excitons self-trapped into the configuration of Ar_2^*) and only thin subsurface layer ~ 100 nm is excited by electrons. In view of relatively low CH_4 content an energy transfer by excitons and holes should be considered in both cases.

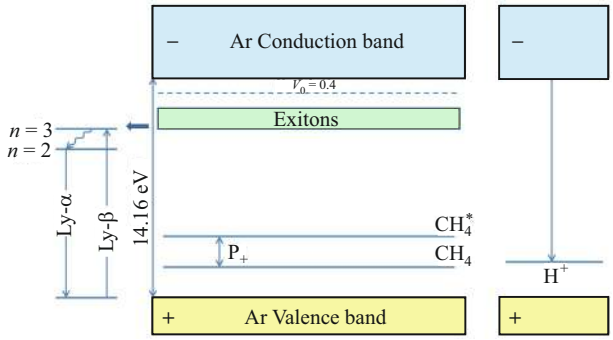

Fig. 7. Energy band scheme of Ar doped with methane and hydrogen atom levels.

Let's discuss possible scenarios for the desorption of excited hydrogen atoms. Figure 7 presents the energy band scheme of Ar doped with CH_4 along with its fragment — H atom.

Because the ionization potential of Ar exceeds the ionization potential of CH_4, efficient charge transfer with the formation of CH_4^+ can occur — the first step of the "hole-induced" scenario (i):

$$Ar^+ + CH_4 \rightarrow Ar + CH_4^+. \quad (5)$$

Deprotonation to the matrix can proceed according to [32] via the reactions:

$$CH_4^+ + h\nu \rightarrow CH_3 + H^+, \quad (6)$$

$$CH_4^+ + h\nu \rightarrow CH_2 + H^+ + H, \quad (7)$$

$$CH_4^+ + h\nu \rightarrow CH + H^+ + 2H, \quad (8)$$

$$CH_4^+ + h\nu \rightarrow CH + H^+ + H_2, \quad (9)$$

$$CH_4^+ + h\nu \rightarrow C + H^+ + 3H, \quad (10)$$

$$CH_4^+ + h\nu \rightarrow C + H_2 + H^+ + H. \quad (11)$$

Then the H^+ proton recombines with the electron, which results in the formation of a highly excited H^{**} atom, followed by its relaxation to the $n = 2$ level and the Ly-α emission by the H^* atom desorbing into the gas phase:

$$H^+ + e^- \rightarrow H^{**} \rightarrow H^* \rightarrow h\nu\,(\text{Ly-}\alpha) + H. \quad (12)$$

It should be pointed out that all of these reactions are endothermic and energy transfer by free excitons can stimulate, in fact, only reaction (7) as follows from an analysis of the breakdown curves [32]. The Branching Ratio (BR) of this reaction with an appearance of H^+, H, and CH_2 products is BR = 0.25 according to [32]. Because of this the contribution of mechanism (i) in the excited H^* atom desorption appeared to be limited.

More effective looks the scenario (ii) based on the dissociative recombination (DR) of CH_4^+ with an electron:

$$CH_4^+ + e^- \rightarrow CH_3 + H\ (0.18 \pm 0.03), \quad (13)$$

$$CH_4^+ + e^- \rightarrow CH_2 + 2H\ (0.51 \pm 0.03), \quad (14)$$

$$CH_4^+ + e^- \rightarrow CH + H_2 + H\ (0.23 \pm 0.01). \quad (15)$$

The BRs of the DR products are shown in parentheses according to the results of experiments performed at the heavy ion storage ring CRYRING [55]. The charge transfer from the Ar hole to the neutral H atom results in a proton formation and its recombination with an electron via Eq. (12).

The desorption scenario (iii) suggests the direct charge transfer from the Ar hole to the H atom appearing at the fragmentation of the neutral CH_4 molecule via Eqs. (1), (3), and (4). Proton formation by this scenario looks quite efficient given high BRs for the H atom formation at an energy of 12.1 eV in Eqs. (1), (3), and (4). BRs in these channels are BR = 0.25, 0.5, and 0.2 respectively [32]. The contribution of secondary products CH_3 and CH_2 in H atom formation is expected to be also high according to [32]. Radiative recombination of H^+ with an electron leads to the population of highly excited H^{**} levels with subsequent relaxation to the excited level $n = 2$ and emission of the Ly-α line upon desorption of H^* atoms [Eq. (12)].

Another conceivable scenario (iv) involves excitons. Taking into account that the $n = 3$ level of hydrogen atom coincides with the exciton band $n = 1$ Γ 3/2 a direct population of the $n = 3$ level is possible followed by relaxation to the $n = 2$ level and the Ly-α emission by desorbing atoms.

Although the desorption of excited H^* atoms has some common features for clusters and solids, there is a pronounced difference in their dynamics. As can be seen from the experimental data presented above small addition of methane (0.1%) to Ar in clusters completely quenched emissions of Ar centers both in the bulk of clusters — band Ar_2^*, and near the surface — band $(Ar_4^+)^*$. Note that the bulk H centers manifesting themselves by the $(Ar_2H)^*$ band at 7.47 eV in the Ar matrix were not observed in the clusters. The reason is believed to lie in the formation of an H atom with an excess of energy (about 1 eV) in all CH_4 fragmentation channels and even 3.1 eV in Eqs. (1) [32], which facilitates the removal of H atoms from the cluster bulk.

In solid matrix at a concentration of CH_4 by two magnitudes higher than that in clusters emission of the matrix, the Ar_2^* band, is still detectable and H centers in the matrix bulk exist in the entire concentration range. The first step in the formation of an excited H^* atom via scenario (iii) is the dissociation of a neutral CH_4 molecule. As it was mentioned the band Ar_2^* falls into CH_4 absorption band, while the band $(Ar_4^+)^*$ is near the onset of absorption [54]. The formation of excited H^* atoms in the "exciton-induced" scenario (iv) is based on the excitation of the ground state H atoms, formed via fragmentation of CH_4 [Eqs. (1), (3), and (4)] or via DR of CH_4^+ (Eqs. (13)–(15)), with excitons. Their production is quite efficient since the diffusion length L_{dif} of therma-lized free excitons in solid Ar $L_{dif} = 12.5$ nm [56, 57] exceeds the distance between the dopants already at $C = 0.1\%$. Note that excitons in Ar clusters with $N \sim 10^3$ atom/cluster were found to be at 12.1 eV according to [58] and can excite an H atom to the $n = 3$ level. The "hole-induced" scenarios (ii) and (iii) involve the charge transfer with the proton formation. Under these scenarios, the H^* atom can be produced via neutralization of the proton only at the fourth and third steps, for (ii) and (iii) cases, respectively. The third step of scenario (i) also involves neutralization of the proton. The existence of slow electrons required for the neutralization reaction was demonstrated in solid Ar doped with CH_4 by observing exoelectron emission [28]. The probabilities of neutralization reaction in the bulk of pure Ar clusters and on their surface differ — neutralization in the bulk is quite efficient, but on the surface, electrons leave the surface [42] that inhibits neutralization reactions and $(Ar_4^+)^*$ centers survive in pure Ar clusters. However, addition of CH_4 molecules completely quenched this band. In view of the low absorbance of CH_4 near 9 eV [54] this fact points to the participation of Ar holes in H^* atoms desorption in clusters. Quenching of both components of Ar emission — neutral Ar_2^* and charged one $(Ar_4^+)^*$, points to the involvement of both scenarios of H^* atoms desorption in clusters: via excitons and holes.

Summary

Comparative study of the electronically stimulated desorption of excited hydrogen atoms H^* from two systems, free nanoclusters Ar/CH_4 and CH_4-doped Ar matrices, was performed. Pure and doped Ar clusters were generated in a supersonic jet. Solid doped matrices were grown on the Cu substrate at LHe temperature. Close-energy electrons were used in the experiments with clusters and solid matrices. The emission spectra were measured in the VUV range, and their transformation caused by doping with CH_4 was investigated. Emission of the desorbing H^* atoms was monitored by the Ly-α line. Registration of the excited state of desorbing atoms made it possible to obtain information on the final stage of relaxation of hydrogen atoms. In combination with an analysis of energy transfer paths, this allowed us to reconstruct scenarios of electronically induced desorption of H^* atoms.

Four scenarios of the excited H^* atoms desorption from clusters and Ar matrix are suggested: (i), (ii), and (iii) via holes, and (iv) via excitons. The first three scenarios for the generation of an excited hydrogen atom H^* in a matrix or Ar cluster have a common last stage – neutralization of the proton $H^+ + e^- \rightarrow H^{**} \rightarrow H^* \rightarrow$ Ly-α. However, the ways of proton formation are different. In scenario (i) H^+ appears due to deprotonation to the matrix. The second scenario (ii) assumes dissociative recombination of CH_4^+ with the formation of neutral H atoms in the ground state with their subsequent ionization. In the third scenario (iii), neutral H atoms are formed in the ground state by CH_4 fragmentation reactions followed by proton formation. The fourth "exciton-induced" scenario (iv) suggests a direct population of the level $n = 3$ of the H atom by excitons Γ 3/2 with subsequent relaxation to the level $n = 2$ and radiation of the Ly-α line by desorbing into the gas phase H^* atoms.

The appearance of the Ly-α line together with the quenching of the neutral and charged components of the cluster emissions indicates the involvement of both types of the desorption scenarios: via excitons and via holes. The results obtained are of importance for cluster physics, surface science and astrophysical research.

Acknowledgements

The authors cordially thank colleagues Vladimir N. Samovarov, Vladimir E. Bondybey, Oleg Kirichek, Vladimir I. Sugakov, and Hermann Rothard for stimulating discussions.

1. K. Kobayashi, W. D. Geppert, N. Carrasco, N. G. Holm, O. Mousis, M. E. Palumbo, J. H. Waite, N. Watanabe, and L. M. Ziurys, *Astrobiology* **17**, 786 (2017).
2. J. M. Carpenter, *Nature* **330**, 358 (1987).
3. T. L. Scott, J. M. Carpenter, and M. E. Miller, *Preprint* ANL/IPNS/CP-98533 (1999).
4. E. Kulagin, S. Kulikov, V. Melikhov, and E. Shabalin, *Nucl. Instrum. Meth. B* **215**, 181 (2004).
5. O. Kirichek, C. R. Lawson, D. M. Jenkins, C. J. T. Ridley, and D. J. Haynes, *Cryogenics* **88**, 101 (2017).
6. O. Kirichek, C. R. Lawson, G. L. Draper, D. M. Jenkins, D. J. Haynes, and S. Lilley, *JNR* **1**, 1 (2018).
7. E. V. Savchenko, O. Kirichek, C. R. Lawson, I. V. Khyzhniy, S. A. Uyutnov, and M. A. Bludov, *Nucl. Instrum. Meth. B* **433**, 23 (2018).
8. R. N. Clark, R. Carlson, W. Grundy, and K. Noll, *Observed Ices in the Solar System*, in: *The Science of Solar System Ices; Astrophysics and Space Science Library*, M. S. Gudipati and J. Castillo-Rogez (eds.), Springer, New York (2012), Vol. 356, p. 3.
9. T. C. Owen, T. L. Roush, D. P. Cruikshank, J. L. Elliot, L. A. Young, C. de Bergh, B. Schmitt, T. R. Geballe, R. H. Brown, and M. J. Bartholomew, *Science* **261**, 745 (1993).
10. D. P. Cruikshank, T. L. Roush, T. C. Owen, T. R. Geballe, C. de Bergh, B. Schmitt, R. H. Brown, and M. J. Bartholomew, *Science* **261**, 742 (1993).
11. M. E. Brown, C. A. Trujillo, and D. L. Rabinowitz, *ApJ* **635**, L97 (2005).
12. C. J. Bennett, C. S. Jamieson, Y. Osamura, and R. I. Kaiser, *ApJ* **653,** 792 (2006).
13. A. Coupeaud, M. Turowski, M. Gronowski, N. Piétri, I. Couturier-Tamburelli, R. Kołos, and J.-P. Aycard, *J. Chem. Phys.* **126**, 164301 (2007).
14. Y.-J. Wu, H.-F. Chen, C. Camacho, H. A. Witek, S.-C. Hsu, M.-Y. Lin, S.-L. Chou, J. F. Ogilvie, and B.-M. Cheng, *ApJ* **701**, 8 (2009).
15. J. He, K. Gao, G. Vidali, C. J. Bennett, and R. I. Kaiser, *ApJ* **721**, 1656 (2010).
16. J. F. Ogilvie, S-L. Chou, M-Y. Lin, and B-M. Cheng, *Vib. Spectrosc.* **57**, 196 (2011).
17. Ch. K. Materese, D. P. Cruikshank, S. A. Sandford, H. Imanaka, and M. Nuevo, *ApJ* **812**, 150 (2015).
18. K. I. Öberg, *Chem. Rev.* **116**, 9631 (2016).
19. F. A. Vasconcelos, S. Pilling, W. R. M. Rocha, H. Rothard, and P. Boduch, *ApJ* **850**, 174 (2017).
20. S. Esmaili, A. D. Bass, P. Cloutier, L. Sanche, and M. A. Huels, *J. Chem. Phys*. **147**, 224704 (2017).
21. M. J. Abplanalp, B. M. Jones, and R. I. Kaiser, *Phys. Chem. Chem. Phys.* **20**, 543 (2018).
22. T. Custer, U. Szczepaniak, M. Gronowski, N. Piétri, I. Couturier-Tamburelli, J.-C. Guillemin, M. Turowski, and R. Kołos, *Phys. Chem. Chem. Phys.* **21**, 13668 (2019).
23. E. Savchenko, I. Khyzhniy, S. Uyutnov, M. Bludov, G. Gumenchuk, and V. Bondybey, *Nucl. Instrum. Meth. B* **460**, 244 (2019).
24. J. Eberlein and M. Creuzburg, *Mol. Phys.* **96**, 451 (1999).
25. D. E. Milligan and M. E. Jacox, *J. Chem. Phys*. **47**, 5146 (1967).
26. M.-Y. Lin, J.-I. Lo, H.-C. Lu, S.-L. Chou, Y.-C. Peng, B.-M. Cheng, and J. F. Ogilvie, *J. Phys. Chem. A* **118**, 3438 (2014).
27. J.-I. Lo, M.-Y. Lin, Y.-C. Peng, S.-L. Chou, H.-C. Lu, B.-M. Cheng, and J. F. Ogilvie, *MNRAS* **451**, 159 (2015).
28. I. V. Khyzhniy, S. A. Uyutnov, M. A. Bludov**,** E. V. Savchenko, and V. E. Bondybey, *Fiz. Nizk. Temp*. **45**, 843 (2019) [*Low Temp. Phys*. **45**, 721 (2019)].
29. E. Savchenko, I. Khyzhniy, S. Uyutnov, M. Bludov, and V. Bondybey, *Nucl. Instrum. Meth. B* **469**, 37 (2020).
30. E. V. Savchenko, I. V. Khyzhniy, S. A. Uyutnov, M. A. Bludov, and V. E. Bondybey, *J. Mol. Struct.* **1221**, 128803 (2020).
31. M.-Y. Song, J.-S. Yoon, H. Cho, Y. Itikawa, G. P. Karwasz, V. Kokoouline, Y. Nakamura, and J. Tennyson, *J. Phys. Chem. Ref. Data* **44**, 023101 (2015).
32. T. IdBarkach, M. Chabot, K. Béroff, S. Della Negra, J. Lesrel, F. Geslin, A. Le Padellec, T. Mahajan, and S. Díaz-Tendero, *A&A* **628**, A75 (2019).
33. K. Vaskonen, J. Eloranta, T. Kiljunen, and H. Kunttu, *J. Chem. Phys*. **110**, 2122 (1999).
34. V. I. Feldman, F. F. Sukhov, and A. Y. Orlov, *J. Chem. Phys.* **128**, 214511 (2008).
35. G. K. Oserov, D. S. Bezrukov, and A. A. Buchachenko, *Fiz. Nizk. Temp.* **45**, 347 (2019) [*Low Temp. Phys*. **45**, 301 (2019)].
36. M. Kraas and P. Gurtler, *Chem. Phys. Lett*. **174**, 396 (1990).
37. M. A. Allodi, R. A. Baragiola, G. A. Baratta, M. A. Barucci, G. A. Blake, J. R. Brucato, C. Contreras, S. H. Cuylle, Ph. Boduch, D. Fulvio, M. S. Gudipati, S. Ioppolo, Z. Kaňuchová, A. Lignell, H. Linnartz, M. E. Palumbo, U. Raut, H. Rothard, F. Salama, E. V. Savchenko, E. Sciamma-O'Brien, and G. Strazzulla, *Space Sci. Rev*. **180**, 101 (2013).
38. E. V. Savchenko, G. Zimmerer, and V. E. Bondybey, *J. Lumin.* **129**, 1866 (2009).
39. E. V. Savchenko, A. G. Belov, G. B.Gumenchuk, A. N. Ponomaryov, and V. E. Bondybey, *Chem. Phys*. **9**, 1329 (2007).
40. I. V. Khyzhniy, S. A. Uyutnov, M. A. Bludov, and E. V. Savchenko, *Fiz. Nizk. Temp*. **44**, 1565 (2018) [*Low Temp. Phys*. **44**, 1223 (2018)].
41. M. A. Bludov, I. V. Khyzhniy, E. V. Savchenko, V. I. Sugakov, and S. A. Uyutnov, *Nucl. Phys. At. Energy* **21**, 312 (2020).

42. E. T. Verkhovtseva, E. A. Bondarenko, and Yu. S. Doronin, *Fiz. Nizk. Temp*. **30**, 47 (2004) [*Low Temp. Phys.* **30**, 34 (2004)].
43. Yu. S. Doronin and V. N. Samovarov, *Fiz. Nizk. Temp*. **32**, 337 (2006) [*Low Temp. Phys*. **32**, 251 (2006)].
44. O. P. Konotop, S. I. Kovalenko., O. G. Danylchenko, and V. N. Samovarov, *J. Clust. Sci*. **26**, 863 (2015).
45. R. Karnbach, M. Yoppien, J. Stapelfeldt, J. Wörmer, and T. Möller, *Rev. Sci. Instrum.* **64**, 2838 (1993).
46. K. S. Song and R. T. Williams, *Self-Trapped Excitons*, Springer-Verlag, Berlin (1996).
47. M. Kraas and P. Gurtler, *Chem. Phys. Lett*. **183**, 264 (1991).
48. M. Kraas and P. Gurtler, *Chem. Phys. Lett*. **187**, 527 (1991).
49. A. G. Belov, M. A. Bludov, and E. I. Tarasova, *Fiz. Nizk. Temp*. **35**, 1230 (2009) [*Low Temp. Phys*. **35**, 957 (2009)].
50. A. Adams and P. K. Hansma, *Phys. Rev. B* **22**, 4258 (1980).
51. E. A. Bondarenko, E. T. Verkhovtseva, Yu. S. Doronin, and A. M. Ratner, *Chem. Phys. Lett*. **182**, 637 (1991).
52. R. Müller, M. Joppien, and T. Möller. *Z. Phys. D* **26**, 370 (1993).
53. E. V. Savchenko, I. V. Khyzhniy, S. A. Uyutnov, G. B. Gumenchuk, A. N. Ponomaryov, M. K. Beyer, and V. E. Bondybey, *J. Phys. Chem. A* **115**, 7258 (2011).
54. Y.-J. Wu, C. Y. R. Wu, S.-L. Chou, M.-Y. Lin, H.-C. Lu, J.-I. Lo, and B.-M. Cheng, *ApJ* **746**, 175 (2012).
55. R. D. Thomas, I. Kashperka, E. Vigren, W. D. Geppert, M. Hamberg, M. Larsson, M. Af Ugglas, V. Zhaunerchyk, *J. Phys. Chem. A* **117**, 9999 (2013).
56. I. Ya. Fugol', *Adv. Phys*. **37**, 1 (1988).
57. A. F. Coletti, J. M. Debever, and G. Zimmerer, *J. Physique Lett.* **45**, 467 (1984).
58. J. Wörmer, M. Joppien, G. Zimmerer, and T. Möller, *Phys. Rev. Lett*. **67**, 2053 (1991).

Десорбція збуджених атомів H^* з вільних кластерів Ar/CH_4 та твердого Ar, який допований CH_4

Yu. S. Doronin, V. L. Vakula, G. V. Kamarchuk, A. A. Tkachenko, I. V. Khyzhniy, S. A. Uyutnov, M. A. Bludov, E. V. Savchenko

Десорбція збуджених атомів водню була виявлена як з твердого Ar, допованого CH_4, так і з вільних нанокластерів Ar/CH_4 при опроміненні електронним пучком. Десорбцію відстежували за лінією Ly-α. Вимірювання спектрів катодолюмінесценції (КЛ) у діапазоні ВУФ проводили в межах концентрацій CH_4 0,1–10 % у твердій матриці. КЛ вільних кластерів із середнім розміром 1200 атомів на кластер реєстрували з чистого кластерного струменя Ar та з кластерів Ar, допованих 0,1 % CH_4. На основі аналізу шляхів передачі енергії з кінцевою стадією релаксації — заселенням $n = 3$ стану атомів водню, запропоновано механізми десорбції електронно-збуджених атомів H^* з твердих тіл і кластерів.

Ключові слова: водень, ізоляція матриці, кластери, електронне опромінення, люмінесценція, десорбція.